NOISE-FREE STOCHASTIC RESONANCE IN A MODEL FOR SPATIOTEMPORAL TURBULENCE*

A. Krawiecki

Faculty of Physics, Warsaw University of Technology
Koszykowa 75, 00-662 Warsaw, Poland

(Received October 1, 2002)

Noise-free stochastic resonance is demonstrated numerically in a model for Rayleigh–Bénard turbulence in a spatially extended system, based on a one-dimensional array of coupled chaotic Lorenz cells. The system shows spatiotemporal intermittency as the control parameter — equivalent to the temperature difference between the upper and lower surface of the liquid layer — is increased. If the temperature difference is slowly modulated periodically, the signal-to-noise ratio, obtained from the output signal reflecting the occurrence of laminar and turbulent phases in a given point in space, shows maximum as a function of the mean value of the control parameter. The results suggest that experimental observation of noise-free stochastic resonance in spatially extended systems is possible.

PACS numbers: 05.45.–a, 47.52.+j, 05.40.–a

1. Introduction

Stochastic resonance (SR) is a phenomenon occurring in systems driven by a combination of a periodic signal and noise, in which the strength of a periodic component of a suitably defined output signal is maximum for optimum nonzero noise intensity [1] (for review see [2–4]). For example, in a generic model for SR, jumps of a particle, subject to a weak periodic force and optimum noise, between symmetric wells of a bistable potential can exhibit noticeable periodicity [1,5]. A separate class of systems with SR is formed by chaotic models in which, instead of external noise, the internal chaotic dynamics can be tuned to maximize the periodic component of the output signal. This is achieved by varying a control parameter, and the corresponding phenomenon is called noise-free (dynamical) SR [6–11]. The strength of the periodic component of the output signal can be expressed as,

* Presented at the XV Marian Smoluchowski Symposium on Statistical Physics, Zakopane, Poland, September 7–12, 2002.

e.g., the signal-to-noise ratio (SNR) in dB at the frequency of the periodic signal ω_0, defined as $\mathrm{SNR} = 10\log S_P(\omega_0)/S_N(\omega_0)$. Here, $S(\omega)$ denotes the power spectral density (PSD) of the output signal, and $S_P(\omega_0)$ is the height of the peak in the PSD at ω_0, above the noisy background in the vicinity of ω_0, which is denoted as $S_N(\omega_0)$. Then the hallmarks of SR and noise-free SR are that the SNR has a maximum as a function of the input noise intensity or the control parameter, respectively. In recent years, an important topic has been investigation of SR in spatially extended stochastic systems [12–20]. For example, in arrays of coupled elements exhibiting SR enhancement of the maximum SNR due to proper coupling in comparison with that in an uncoupled element, and its increase with the size of the array were found [12–17]. This effect, known as array-enhanced SR, appears because the noise and coupling can synchronize the output signals of all elements with the periodic signal, so that the latter is best reflected in the dynamics of the elements in the array. In other cases, SR appears since the system provides space for two stable extended configurations, corresponding to two wells of the bistable potential in the above-mentioned generic model for SR [18–20], *e.g.*, two pinning points for a soliton in a one-dimensional medium [19, 20].

In this paper the study of SR-like phenomena is extended to the case of noise-free SR in spatially extended chaotic systems. A typical route to chaos in spatially extended systems is spatiotemporal intermittency (STI) [21–31]. As the control parameter is increased, isolated turbulent domains appear on the laminar background; for still higher values of the control parameter these domains grow in size and can be spontaneously created and annihilated; eventually, all turbulent domains are connected and the system becomes mostly turbulent. STI has been predicted theoretically in coupled map lattices [21] and partial differential equations [22], and observed experimentally, *e.g.*, in Rayleigh–Bénard convection [23, 24], turbulent regimes of lines of electromagnetically forced vortices [28], Taylor–Couette flow [29], and dynamics of self-excited ionization waves [31]. A strong analogy between STI and directed percolation has been conjectured, although there has been a long debate if both phenomena belong to the same universality class [22, 27, 30]. In Ref. [7] it was proved that low-dimensional chaotic systems with intermittency can exhibit noise-free SR: information about the driving periodic signal can be reflected in the sequence of laminar phases and bursts, which play a role of the two stable states in the generic bistable model for SR. This sequence shows maximum periodicity for the optimum value of the control parameter. This paper is aimed to show that, similarly, in spatially extended systems with STI information about the periodic signal can be best encoded in the sequence of laminar and turbulent domains for the optimum value of the control parameter.

For this purpose, numerical simulations of a one-dimensional array of coupled chaotic Lorenz systems [32] are performed, each consisting of three nonlinear ordinary differential equations. This approximate model [26] was introduced to describe experiments with Rayleigh–Bénard convection in a fluid layer between horizontal boundaries, of which the lower one is heated from below. The model was shown to reproduce, at least qualitatively, certain experimental results, as the transition to spatiotemporal chaos via STI, and the statistical distributions of the lengths of laminar domains both below and above the threshold for fully developed turbulence. In this paper, a small periodic modulation is added to one of the model parameters, equivalent to periodic modulation of the temperature difference between the lower and upper boundary. It is found that when the mean value of the temperature difference, playing a role of the control parameter, is optimum, the SNR measured from the signal reflecting the occurrence of a laminar or turbulent phase at a certain point in space is maximum. In this way, noise-free SR in a system with STI is demonstrated. Dependence of this phenomenon on the system size and possible experimental realizations are briefly discussed.

2. The model

In the Rayleigh–Bénard experiment a layer of fluid is confined between two horizontal plates and heated from below [23, 24]. As the temperature difference ΔT between the plates increases, a steady convective flow is observed, which for small system size has a form of a one-dimensional chain of vertical vortices, with neighboring vortices rotating in opposite directions. For higher ΔT this structure is destroyed by the appearance of small, localized in space turbulent domains in which the spatial periodicity is violated, surrounded by large laminar domains in which the chain of vortices is still periodic. With increasing temperature difference the turbulent regions migrate and invade the laminar ones, and the portion of the system occupied by the turbulent domains grows. This route to turbulence is typical of STI and shows some evidence for a second-order phase transition, though in the case of annular system geometry (periodic boundary conditions for the flow) this transition need not be perfect [24].

The Lorenz model [32] is a drastic simplification of the Navier–Stokes equations for the problem of Rayleigh–Bénard convection, obtained by retaining only three spatial Fourier coefficients of the fluid velocity and temperature. In order to model a spatially extended fluid layer, in Ref. [26] it was assumed that the basic structure of the fluid motion in the Rayleigh–Bénard experiment consists of vortices which persist for a range of ΔT that includes turbulent behavior. Each vortex, or cell, was then modeled by a single Lorenz system, and the cells were coupled by viscous effects and thermal coupling. This led to the following system of coupled ordinary differential equations

$$\begin{aligned} \dot{x}_i &= \sigma\left(y_i - x_i\right) - \mu\left(x_{i-1} + 2x_i + x_{i+1}\right) , \\ \dot{y}_i &= -y_i + \left(r - z_i\right) x_i - \kappa\left(y_{i-1} + 2y_i + y_{i+1}\right) , \\ \dot{z}_i &= x_i y_i - b z_i , \end{aligned} \tag{1}$$

where $i = 1, 2, \ldots N$ is the cell index, the significant variables x_i and y_i are related to the fluid velocity and temperature in each cell, μ is the strength of viscous force at the interface between adjacent cells, assumed in the form $\mu\left[x_i\left(t\right) + x_{i+1}\left(t\right)\right]$, κ is the strength of thermal coupling by heat exchange between adjacent cells, and the significant parameter r is proportional to the temperature difference between the lower and upper boundary ΔT. The meaning of the remaining variables and parameters is given in Ref. [26]. Note that the viscous force is minimum when x_i and x_{i+1} have opposite signs, which amounts to the opposite direction of fluid rotation in neighboring vortices. In experiments the latter situation is typical of laminar domains, while in turbulent domains the vortices rotate in the same direction. Thus in the model (1) a given cell i is classified as belonging at time t to a turbulent domain if $x_{i-1}(t)x_i(t) > 0$ or $x_i(t)x_{i+1}(t) > 0$; otherwise it is classified as belonging to a laminar domain. Following Ref. [26], henceforth the thermal coupling between adjacent cells is neglected by setting $\kappa = 0$. If the parameters σ, b are assumed such that the uncoupled Lorenz system can show deterministic chaos for a certain range of r, then with $\mu > 0$ and increasing r transition to turbulence via the appearance of turbulent domains and STI is observed in the model (1).

In order to investigate noise-free SR a small, slowly varying input periodic signal with frequency $\omega_0 \ll 1$ and amplitude r_1 was added in Eq. (1) to the constant in time part of the control parameter r_0,

$$r \to r(t) = r_0 + r_1 \cos\left(\omega_0 t\right) , \tag{2}$$

which amounts to a small periodic modulation of the temperature difference between the upper and lower layer ΔT. The system of Eq. (1) and (2) was simulated numerically with periodic boundary conditions, equivalent to the annular geometry in experiments, and with various even N which allows the period-2 laminar phase. The output signal $Y(t)$ was obtained from the time series of the middle cell, *i.e.*, that with $i = N/2$, and defined so that to distinguish if the cell was turbulent ($Y(t) = 1$) or laminar ($Y(t) = 0$); such a two-state reduction of the output signal is typical of SR [5]. Note that the output signal reflected the local dynamics at a given site, in analogy with the numerical simulations of SR in arrays of coupled stochastic systems [12], rather than the average or complete dynamics of the whole system. As a measure of the noise-free SR the output SNR *vs* the control parameter r_0 was investigated.

3. Numerical results and discussion

The system (1) was solved numerically using a fourth-and-fifth order Runge–Kutta method with continuous control of the integration step size, with parameters $\sigma = 10$, $b = 8/3$, $\mu = 3$, $r_1 = 4$, $\omega_0 = 2\pi \times 2^{-13}$, and varying r_0, for $4 \leq N \leq 128$. The SNR obtained numerically was normalized to

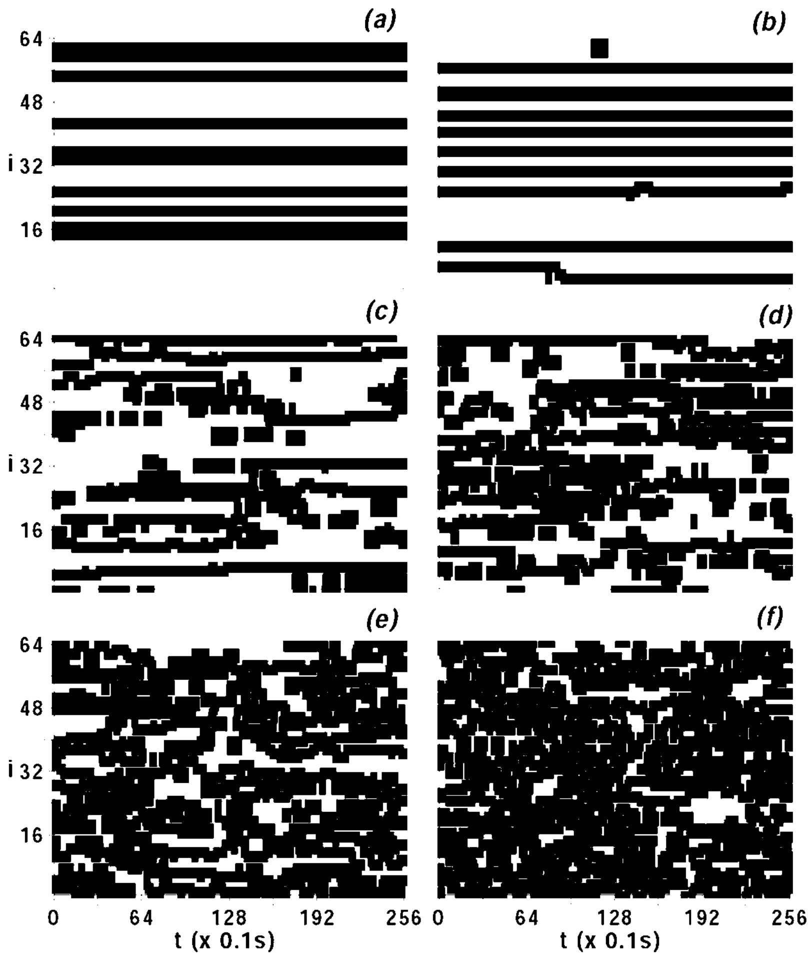

Fig. 1. Spatiotemporal diagrams for the system (1) with $N = 64$ and $r = \text{const}$, for $r = 23$ (a), $r = 29$ (b), $r = 35$ (c), $r = 39$ (d), $r = 43$ (e), $r = 51$ (f). Black points denote turbulent cells, white points denote laminar cells.

the frequency bandwidth [5] $\Delta f = \omega_0/(2\pi M)$, where M is the number of periods of the input signal during which the data were stored (in the present simulations, $M = 32$ was used). The results were then averaged over several hundreds of the stored time series.

Without periodic modulation, for $r_1 = 0$, the system (1) shows transition to spatiotemporal chaos via the STI as r is increased for a whole range of N studied (Fig. 1 and Fig. 2). In Fig. 1 (where $N = 64$) the transition to fully developed turbulence, when all turbulent domains are connected, occurs between $r = 39$ (Fig. 1(d)) and $r = 43$ (Fig. 1(e)). The exact threshold for turbulence is hard to establish; the transition is confirmed by different scaling behavior of the distribution of lengths of laminar domains far below and above the threshold [26]. The simulations reveal that the thresholds for the spontaneous creation of turbulent domains and for the transition to turbulence slightly increase for small N. For example, for $r = 29$ and $N = 16$ the turbulent domains are still localized (Fig. 2(b)), while for $N = 64$ they already start invading the laminar domains (Fig. 1(b)). Nevertheless, qualitative changes of the system dynamics with increasing r and the overall picture of the STI are independent of N (*cf.* Fig. 1 and Fig. 2).

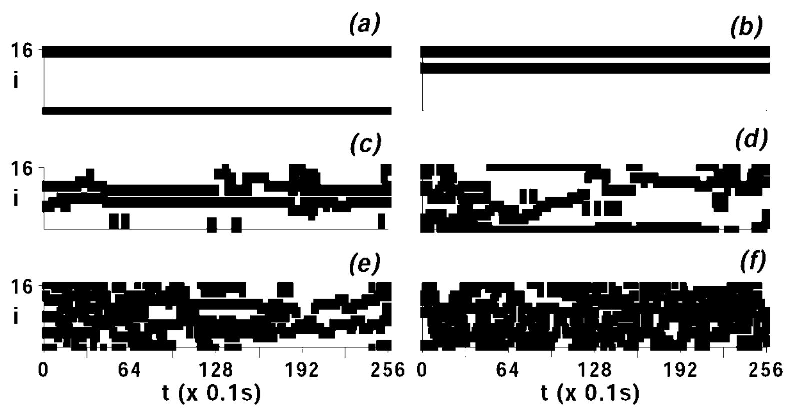

Fig. 2. Spatiotemporal diagrams for the system (1) with $N = 16$ and $r = \text{const}$, for $r = 23$ (a), $r = 29$ (b), $r = 35$ (c), $r = 39$ (d), $r = 43$ (e), $r = 51$ (f). Black points denote turbulent cells, white points denote laminar cells.

In the case of the time-dependent control parameter (2), the portion of the system occupied by the turbulent regions can change significantly as $r(t)$ varies between its maximum and minimum value. This happens when $r_0 \pm r_1$ is, approximately, between the threshold for the spontaneous creation and annihilation of turbulent domains and that for the fully developed turbulence. Then the periodicity of $r(t)$ is well reflected in the sequence of turbulent and laminar domains in the spatiotemporal diagrams in Fig. 3, which play a role analogous to that of the two stable states in models for SR with bistable potentials. For example, the overall laminar behavior can be periodically interrupted by time intervals during which the turbulent domains prevail (Fig. 3(b), (c)). Another possibility is that the system is mostly turbulent, and intervals during which the system is more laminar

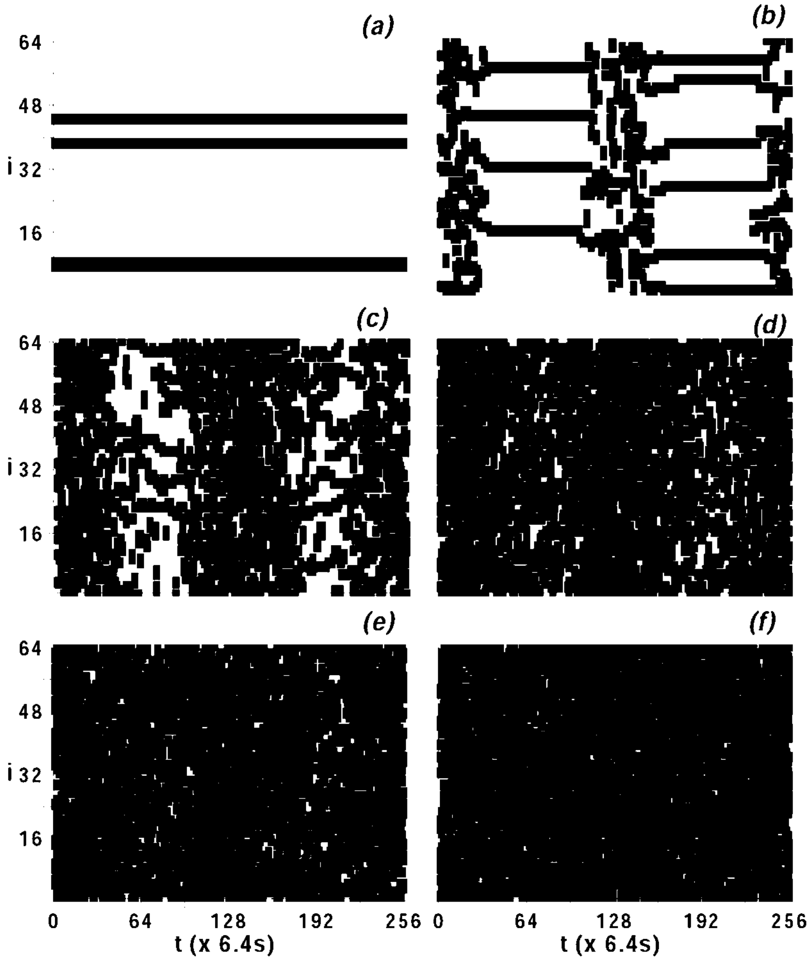

Fig. 3. Spatiotemporal diagrams for the system (1) with the time-dependent control parameter (2), $N = 64$, and $r_0 = 23$ (a), $r_0 = 29$ (b), $r_0 = 35$ (c), $r_0 = 39$ (d), $r_0 = 43$ (e), $r_0 = 51$ (f). Black points denote turbulent cells, white points denote laminar cells. Diagrams (c)–(e) correspond to the range of r_0 in which the maximum of the SNR in Fig. 4 appears. Note different time scales on the horizontal axes in comparison with Fig. 1 and 2.

appear periodically on this background (Fig. 3(d)). For optimum r_0 the periodicity of $r(t)$ is also best reflected in the output signal $Y(t)$ from a single Lorenz cell. For any system size, the SNR measured from $Y(t)$ has a maximum as a function of r_0 (Fig. 4(a)). The maximum appears in the range of r_0 for which the transition to fully developed turbulence takes place. This shows that information about the input signal can be encoded in the sequence of laminar and turbulent phases at a single site, and that for the optimum value of r_0 this encoding is also optimum, *i.e.*, that noise-free SR in the spatially extended system with STI appears.

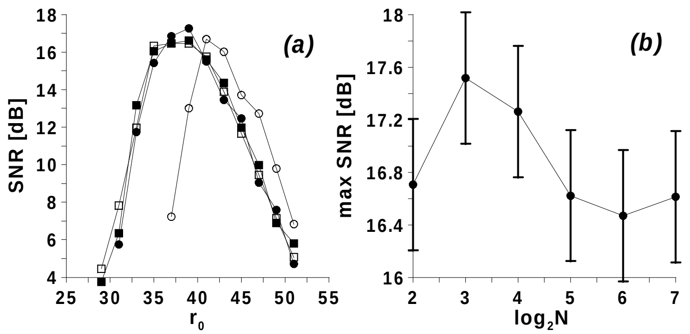

Fig. 4. (a) The signal-to-noise ratio SNR *vs* r_0 for the system (1,2) with $\omega_0 = 1/8192$, $r_1 = 4$, and $N = 4$ (empty circles), $N = 16$ (filled circles), $N = 64$ (empty squares), $N = 128$ (filled squares); (b) maximum SNR *vs* N for the system as in (a).

While the location of the maximum SNR slightly depends on the system size, in particular for small N (Fig. 4(a)), its height is almost independent of N within the measurement accuracy (Fig. 4(b)). In arrays of coupled stochastic bistable oscillators the maximum SNR, measured for both optimum coupling strength and noise intensity, increases with the system size up to saturation [12]. The effect of coupling is to synchronize all oscillators, which strengthens the effect of the external periodic signal; since if one oscillator follows this signal, this increases the probability that its neighbors will also do. In contrast, in the model given by Eq. (1), (2) the spatial extension of the system provides only space for the development and spreading of the laminar and turbulent domains. As mentioned above, the overall picture of the STI, and thus the overall behavior of a single cell, do not depend significantly on the chain length. Thus, the increase of the maximum SNR with N is not observed. Moreover, in the present study the coupling strength is fixed and not necessarily optimum, which can also influence the observed independence of the maximum SNR on the chain length.

4. Summary and conclusions

In this paper the concept of noise-free SR was extended to the case of spatially extended chaotic systems exhibiting generic transition to spatiotemporal chaos via STI. It was shown that the periodic component in the output signal, reflecting the occurrence of the laminar and turbulent phases at a given point in space, can be maximized as a function of the control parameter. The maximum SNR turned out to be rather independent of the system size, because the qualitative picture of the STI, and thus the local dynamics at a single point, did not change much with the spatial extent of the system. Since the model under study is related to the transition to Rayleigh–Bénard turbulence via STI, this suggests a possibility of experimental observation of noise-free SR in experiments analogous to those in Ref. [23, 24], with the periodic signal modulating the temperature difference between the two horizontal boundaries.

The Lorenz cells of the model (1) were low-dimensional chaotic systems, hence the spatially extended array exhibited sustained STI. Sustained STI is also observed in most experiments. The sustained character of intermittency is necessary to observe SR, since turbulent domains have to be continuously created and annihilated following the time variation of the control parameter. In contrast, in many theoretical models for STI the laminar state is absorbing, *i.e.*, only transient STI occurs [21, 22]. This excludes SR in the form discussed in this paper, though it is possible that if the intermittent transient is long enough the input periodic signal will be reflected in the output signal of finite duration.

The phenomenon of SR in one-dimensional stochastic systems is related to the creation of coherent structures (solitons) which, by spreading in the bistable medium, invert its orientation [14]. This bears some resemblance to spontaneous creation of turbulent domains which then invade the laminar ones. It should be also noted that in certain spatially extended systems transition to spatiotemporal chaos occurs via creation and annihilation of solitary waves [33]. If it is possible to observe noise-free SR in such systems, its origin could be more directly related to that of SR with noise in one-dimensional systems.

REFERENCES

[1] R. Benzi, A. Sutera, A. Vulpiani, *J. Phys. A* **14**, L453 (1981).

[2] L. Gammaitoni, P. Hänggi, P. Jung, F. Marchesoni, *Rev. Mod. Phys.* **70**, 223 (1998).

[3] V.S. Anishchenko, A.B. Neiman, F. Moss, L. Schimansky-Geier, *Soviet Physics — Uspekhi* **42**, 7 (1999) [*Usp. Fiz. Nauk* **169**, 7 (1999)].

[4] F. Moss, in: *Self-Organized Biological Dynamics & Nonlinear Control* ed. J. Walleczek, Cambridge University Press, Cambridge, UK, p. 236-256.

[5] B. McNamara, K. Wiesenfeld, *Phys. Rev.* **A39**, 4854 (1989).

[6] V.S. Anishchenko, A.B. Neiman, M.A. Safanova, *J. Stat. Phys.* **70**, 183 (1993).

[7] E. Reibold, W. Just, J. Becker, H. Benner, *Phys. Rev. Lett.* **78**, 3101 (1997).

[8] V.N. Chizhevsky, R. Vilaseca, R. Corbalán, *Phys. Rev.* **E61**, 6500 (2000).

[9] W. Yuqing, Z.D. Wang, W. Wang, *J. Phys. Soc. Japan* **69**, 276 (2000).

[10] S. Matyjaśkiewicz, A. Krawiecki, J.A. Hołyst, K. Kacperski, W. Ebeling, *Phys. Rev.* **E63**, 026215 (2001).

[11] K. Arai, K. Yoshimura, S. Mizutani, *Phys. Rev.* **E65**, 015202 (2002).

[12] J.F. Lindner, B.K. Meadows, W.L. Ditto, M.E. Inchiosa, A.R. Bulsara, *Phys. Rev. Lett.* **75**, 3 (1995); *Phys. Rev.* **E53**, 2081 (1996).

[13] Z. Néda, *Phys. Rev.* **E51**, 5315 (1995); *Phys. Lett.* **A210**, 125 (1996); Kwan-tai Leung, Z. Néda, *Phys. Lett.* **A246**, 505 (1998).

[14] F. Marchesoni, L. Gammaitoni, A.R. Bulsara, *Phys. Rev. Lett.* **76**, 2609 (1996).

[15] P.M. Gade, R. Rai, H. Singh, *Phys. Rev.* **E56**, 2518 (1997).

[16] U. Siewert, L. Schimansky-Geier, *Phys. Rev.* **E58**, 2843 (1998).

[17] A. Krawiecki, A. Sukiennicki, R.A. Kosiński, *Phys. Rev.* **E62**, 7683 (2000).

[18] H.S. Wio, *Phys. Rev.* **E54**, R3075 (1996); B. von Haeften, R. Deza, H.S. Wio, *Phys. Rev. Lett.* **84**, 404 (2000).

[19] J.A. González, B.A. Mello, L.I. Reyes, L.E. Guerro, *Phys. Rev. Lett.* **80**, 1361 (1998).

[20] P. Ruszczyński, L. Schimansky-Geier, I. Dikshtein, *Eur. Phys. J.* **B14**, 569 (2000).

[21] K. Kaneko, *Progr. Theor. Phys.* **74**, 1033 (1985); *Physica D* **37**, 60 (1989); *Phys. Lett.* **A149**, 105 (1990).

[22] H. Chaté, P. Manneville, *Phys. Rev. Lett.* **58**, 112 (1986).

[23] S. Ciliberto, P. Bigazzi, *Phys. Rev. Lett.* **60**, 286 (1988).

[24] F. Daviaud, M. Bonetti, M. Dubois, *Phys. Rev.* **A42**, 3388 (1990).

[25] D. Stassinopoulos, G. Huber, P. Alstrøm, *Phys. Rev. Lett.* **64**, 3007 (1990).

[26] E. Atlee Jackson, A. Kodogeorgiou, *Phys. Lett.* **A168**, 270 (1992).

[27] J.R. deBruyn, L. Pan, *Phys. Rev.* **47**, 4575 (1993).

[28] H. Willaime, O. Cardoso, P. Tabeling, *Phys. Rev.* **E48**, 288 (1993).

[29] P.W. Colovas, C.D. Andereck, *Phys. Rev.* **E55**, 2736 (1997).

[30] J. Rolf, T. Bohr, M.H. Jensen, *Phys. Rev.* **E57**, R2503 (1998).

[31] A. Atipo, G. Bonhomme, T. Pierre, *Eur. Phys. J.* **D19**, 79 (2002).

[32] E.N. Lorenz, *J. Atmos. Sci.* **20**, 130 (1964).

[33] J.J. Żebrowski, *Phys. Rev.* **B39**, 7205 (1989).